

Optimization of parameters affecting the hammer rapping force to ensure the durability of the discharge electrode frame, dust removal acceleration and durability of the collecting electrode plate in the electrostatic precipitator

Tung Nguyen Anh ¹, Phong Phan Dang², Göt Hoang Van ^{3*} and Kien Hoang Trung ⁴

^{1,2,3,4} National Research Institute of Mechanical Engineering, Hanoi, Vietnam

^{2*} Corresponding author

gotnarime@yahoo.com.vn

Abstract. The scientific purpose of this study is to optimize 3 main parameters: hammer mass (m), hammer drop height (h) and filter chamber inlet dust concentration (η) of the Electrostatic precipitator (ESP), to meet the dust removal acceleration (a) and the hammer rapping force (F), ensure the working life span of the discharge electrode frames and the collecting electrode plates. This issue is evaluated as a multi-objective problem. The cyclic impact force (F) not only creates an acceleration (a) to remove the dust from the discharge frame but also causes fatigue damage to important parts of the dust filter chamber such as the discharge frames and collecting plates. To solve the scientific problem mentioned above, the article has applied the standard [2], the theoretical basis of empirical study of the author's [1], experimental results on the static and actual models of the filter chamber, and the theory of fatigue curve construction based on experiments [4,5,6].

Keywords: Dust filter chambers, Hammer rapping system, Discharge electrode.

1 Introduction

Currently, in Vietnamese coal-fired power plants and cement factories, advanced horizontal electrostatic precipitators imported from Germany, France are being popularly utilized [3,4,7,8]. The most important components of the dust filter chamber in ESP are the discharge and collecting electrodes. In which, the collecting electrode plates act as the negative pole and the discharge electrodes in the form of discharge frames fitting with spiked discharge rods act as the positive pole, together ionizing the dust particles passing through the filter chamber [3]. The objective is to gain control of the technology and design of the filter chamber. This article has empirically studied to determine the relationship between the important parameters [1,3,4,7,8] including: hammer rapping force (F), creating dust removal acceleration (a) on the basis of optimizing some technological parameters such as hammer mass (m), drop height of the

hammer (h) and the dust concentration of the inlet flue gas (η) in the filter chamber to ensure the durability of the discharge electrode frame and the collecting plate in the filter chamber of the ESP.

2 Rational of research

According to the Ministry of Construction, nationwide there are currently 29 coal-fired power plants in operation with a total of 58 units, with capacity vary from 200 MW to 600 MW and about 120 coal-fired boilers that emit a large volume of flue gas into the environment. The dust concentration of the flue gas emitted from the boiler is approximately 250 to 350mg/Nm³ and allowable discharge into the environment (depending on specific location of the plant) must be reduced to 50 mg/Nm³ – 100 mg/Nm³ [3,4]. Electrostatic precipitator is the capable equipment to meet the above requirements. The electrodes are supplied with high D.C. voltage ranging from tens to several hundred (kV) [1,4] to form a high intensity electric field. The flue gas stream passes through the filter chamber is ionized by discharge electrode system (positive charged) and microscopic dust particles are attracted to the surface of the collecting plates (negative charged). One of the most important component in the ESP filter chamber is discharge electrodes with frame-discharge rod structure [3,4]. In Vietnam the past decades, ESP equipment has always been imported as synchronous system from abroad. However, recently, the Research Institute of Mechanical Engineering has designed the ESP on the basis of cooperation with foreign suppliers and has manufactured and commissioned the ESPs successfully at Vung Ang 1, Thai Binh 2 and Nghi Son 2 Thermal power plants.

When a discharge electrode frame is damaged, it will lead to stoppage of the plant operation for repair, causing great damage to the power industry. While there are hundreds of active ESPs in the whole country, it is a matter of concern for local scientific researches. Therefore, the research for a scientific solution to determine the appropriate durability of the discharge electrode frame sustaining periodic rapping force (F) that meet the dust removal acceleration (a), and at the same time ensure the durability of the collecting plates [5,6] is currently an urgent issue in Vietnam.

3 Methodology and research

The relationship equation between dust removal acceleration (a), rapping force (F) and influencing parameters (m), (h) and (η) is established by experiment.

3.1 Influencing factors

The influencing factors affecting the durability of the discharge electrode frame and the collecting electrode plates include many factors such as:

- The impact force $F(N)$ of the hammer on the lower beam anvil of the discharge frame every 15 minutes to remove dust is influenced by the hammer mass (m) and the hammer drop height of the hammer (h);

- The dust concentration (η) of flue gas entering the filter chamber ranges from $250\text{mg}/\text{Nm}^3$ to $350\text{mg}/\text{Nm}^3$ after the boiler. According to environmental standard requirements for coal-fired power plants in Vietnam is $50\text{ mg}/\text{Nm}^3$. For one boiler unit capacity of 300MW, the average amount of dust collected in a 15-minute cycle is approximately 200kg.

Practically, for imported ESPs from foreign countries, the parameters of hammer mass (m), hammer drop height (h) and dust accumulated on the frame (η) are selected and optimized to achieve the appropriate operation hammer rapping force (F). Therefore, in this study, three parameters were selected to study are: (m), (h) and (η) to establish the relationship between rapping force (F) of the hammer, hammer mass (m) and drop height (h) and the relationship between dust removal acceleration (a) with 3 parameters: (m); (h) and (η). On the other hand, the rapping force (F) must ensure the dust removal acceleration (a), at the same time satisfying the service life of the discharge frame and the durability of the collecting plate, which is target to be studied.

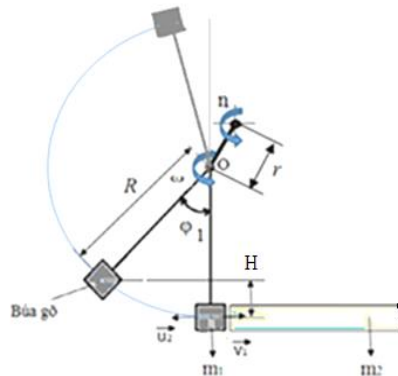


Fig. 1. Impact model of hammer and discharge frame.

3.2 Screening design

Depending on the number of variables to be investigated and the cost and time requirements for the experiment, select the L9 type experiment design for screening design plan. In order to improve the reliability of the experiments, repeat some selected experiments one more time if necessary. Thus, the L9 type exploratory experiment design was selected, in which includes 3 central experiments. From the experimental results, the below matrix is documented (tables 1 and 3).

Table 1. Exploratory matrix for 3 factors

m	h	η	a_{tt}	F_{tn}
-----	-----	--------	----------	----------

6	0.53	350	2908	492.53
6	0.53	250	2877	481.81
6	0.49	250	2831	472.32
9	0.53	350	3455	549.77
9	0.49	250	3239	535.25
9	0.49	350	3258	541.49
6	0.49	350	2803	469.32
9	0.53	250	3417	542.08

Table 2. Input parameters

Parameter	Symbol	Unit	Value level		
			1	2	3
Hammer mass	m	kg	6	7	8
Drop height between hammer center and impact point	h	m	0.49	0.53	0.57
Dust concentration	η	(mg/Nm ³)	250	300	350

Table 3. Experimental matrix and result for dust removal acceleration

No.	m (kg)	h (m)	η (mg/Nm ³)	Dust removal acceleration a (m/s ²)
1	6	0.49	250.00	2831.00
2	6	0.53	300.00	2905.77
3	6	0.57	350.00	3064.95
4	7	0.49	300.00	2888.66
5	7	0.53	350.00	3203.55
6	7	0.57	250.00	3121.00
7	8	0.49	350.00	3201.75
8	8	0.53	250.00	3239.00
9	8	0.57	300.00	3270.26
10	8	0.57	350.20	3510.00
11	8	0.57	349.15	3495.00
12	8	0.57	350.15	3505.00

In Figure 2, three effect graphs of 3 variables are plotted in independent plots. The upper left corner of the graph shows the influence of the mass variable of the hammer (m), observed on the graph, when m changes from 6kg to 8kg, the graph (a) is steepest among the factors, the objective function varies from 2920 (m/s²) to 3275(m/s²). The slope of this graph is $(3275-2920)/2 = 177.5$. By qualitative comparison shows that the slope of the influence graph of (m) is the largest; next is the graph of (h) with slope $(3210-2970)/2 = 120$ and finally η has slope $(3110-3090)/2 = 10$. The greater

the slope of the graph, the greater the influence of the variable plotted on that graph to the objective function. Thus, the variable (m) has the strongest influence on the objective function; and variable (η) has the weakest effect.

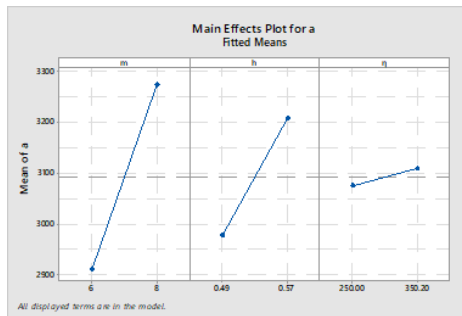


Fig. 2. Main factor affecting the dust removal acceleration plot

Another way to evaluate the main effects is to look at the standardized effects graph or the Pareto effects graph.

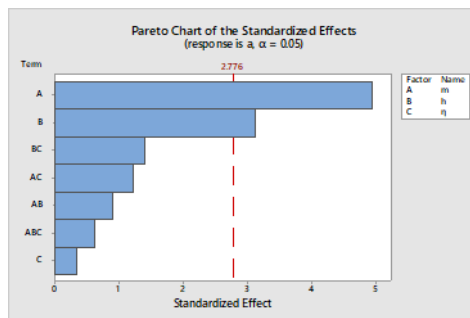


Fig. 3. Pareto chart for the factors affecting the dust removal acceleration (a)

On the graph in Figure 3, Minitab uses the significance level value α to indicate the limit line (with coordinates 2.776 on the graph) of the reversed null hypothesis area. The influence values (standardized) are presented as horizontal bars. The factors corresponding to the bar represented to the right of the limit line are values with significant influence. The factors represented to the left of the limit line are weakly influential.

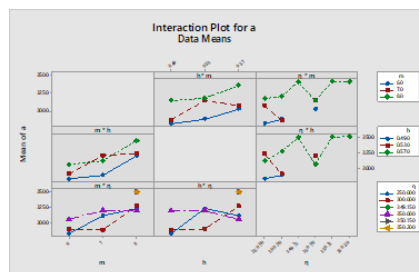


Fig. 4. Pareto chart for the factors affecting the dust removal acceleration (a)

The graph shows that the factors: A (variable m), B (variable h) have values beyond the limit line. Interaction effects will be analyzed in more detail in the next section. Thus, two experimental variables m and h have a great influence on the objective function. This is consistent with the conclusions drawn from the graph analysis of the main influencing factors (Figure 4).

From the graph it is shown that:

- Consider the second cell in the first row: it can be seen that when rapping with a hammer mass $m = 6\text{kg}$, the value of the objective function (a) increases when (h) increases from 0.49m to 0.53m and increases sharply if (h) increases from 0.53m to 0.57m; but if rapping with a 7kg hammer, the objective function value increases when (h) increases from 0.49m to 0.53m, however (a) will decrease if it continues to increase from 0.53m to 0.57m. On the graph, the dashed line is steeper than the solid line. This means, whether (m) is large or small, it will affect the effect of the variable (h) on the objective function (a). In other words, (m) has a significant interaction effect and then the effect of (h).

- The same procedure was conducted to the remaining effect.

ANOVA for Regression

Table 4. Experimental matrix and result for dust removal acceleration

Source	DF	Adj SS	Adj MS	F-Value	P-Value
Model	7	602327	86047	15.51	0.009
Linear	3	238883	79628	14.35	0.013
m	1	135467	135467	24.41	0.008
h	1	54044	54044	9.74	0.036
η	1	650	650	0.12	0.749
2-Way Interactions	3	16676	5559	1.00	0.478
m*h	1	4522	4522	0.81	0.418
m* η	1	8223	8223	1.48	0.290
h* η	1	10764	10764	1.94	0.236
3-Way Interactions	1	2133	2133	0.38	0.569
m*h* η	1	2133	2133	0.38	0.569
Error	4	22198	5549		
Total	11	624525			

Table 5. Model Summary

S	R-sq	R-sq (adj)	R-sq (pred)
74.4944	96.45%	90.23%	0.00%

Firstly, by observing the regression model, it is shown that the coefficients of the variables (m) and (h) have very small (p) values. That proves the presence of these two variables in the regression equation is significant. The other variables and interactions all have p-values much larger than the significance level $\alpha=0.05$, so they can be removed from the regression equation. The analysis of variance shows that the probability (p) value corresponding to the main effects is small (0.013). Therefore, the effects of the variables are significant. Two-way interactions (2-way Interactions) have a p-value of 0.478 and 3-way interactions (3-way Interactions) have a p-value of 0.569 which is much larger than the level α (0.05). Therefore, it can be asserted that the variables have a relatively small interaction effect.

3.3 Experiment planning 3^3

a) Design the 3^3 matrix: After the exploration step, it can be confirmed that the 3 main factors affecting the dust removal acceleration are hammer mass (m), hammer drop height (h), and dust concentration (η). On the other hand, on the basis of experimental results with hammer weight ranges from 6kg to 9kg, the maximum tensile stress σ_{\max} at the dangerous point of the frame has been calculated, showing that when $m=9\text{kg}$, σ_{\max} is larger than the allowable stress of the material CT3 steel of the discharge frame: $\sigma_{\max} \leq [\sigma]=240\text{MPa}$. Therefore, for the experimental matrix planning, the hammer mass is limited from 6 to 8 kg. Exploratory empirical matrix with 3 factors allows the establishment of an exploratory matrix (Table 6).

Table 6. Empirical matrix 3^3

No.	Variable			Coded variable			Average acceleration
	m	h	η	X1	X2	X3	a
1	6	0.49	250	-1	-1	-1	2831
2	6	0.49	300	-1	-1	0	2888
3	6	0.49	350	-1	-1	1	2803
4	6	0.53	250	-1	0	-1	2877
5	6	0.53	300	-1	0	0	2906
6	6	0.53	350	-1	0	1	2908
7	6	0.57	250	-1	1	-1	2919
8	6	0.57	300	-1	1	0	2890
9	6	0.57	350	-1	1	1	3065
10	7	0.49	250	0	-1	-1	2978
11	7	0.49	300	0	-1	0	2889
12	7	0.49	350	0	-1	1	2859
13	7	0.53	250	0	0	-1	3051
14	7	0.53	300	0	0	0	3020
15	7	0.53	350	0	0	1	3204

16	7	0.57	250	0	1	-1	3121
17	7	0.57	300	0	1	0	3177
18	7	0.57	350	0	1	1	3207
19	8	0.49	250	1	-1	-1	3105
20	8	0.49	300	1	-1	0	3160
21	8	0.49	350	1	-1	1	3202
22	8	0.53	250	1	0	-1	3239
23	8	0.53	300	1	0	0	3304
24	8	0.53	350	1	0	1	3327
25	8	0.57	250	1	1	-1	3337
26	8	0.57	300	1	1	0	3270
27	8	0.57	350	1	1	1	3404

b) Analysis of Variance and Regression Equation:

Table 7. Analysis of Variance

Source	DF	Adj SS	Adj MS	F-Value	P-Value
Model	7	781533	111648	33.06	0.000
Linear	3	762189	254063	75.23	0.000
m	1	591042	591042	175.02	0.000
h	1	156116	156116	46.23	0.000
η	1	15031	15031	4.45	0.048
2-Way Interactions	3	14128	4709	1.39	0.275
m*h	1	3058	3058	0.91	0.353
m* η	1	878	878	0.26	0.616
h* η	1	10193	10193	3.02	0.099
3-Way Interactions	1	5216	5216	1.54	0.229
m*h* η	1	5216	5216	1.54	0.229
Error	19	64164	3377		
Total	26	845697			

Table 8. Model Summary

S	R-sq	R-sq (adj)	R-sq (pred)
58.1122	92.41%	89.62%	87.24%

Table 9. Analysis of Variance

Term	Effect	Coef	SE Coef	T-Value	P-Value	VIF
Constant		3071.8	11.2	274.67	0.000	

m	362.4	181.2	13.7	13.23	0.000	1.00
h	186.3	93.1	13.7	6.80	0.000	1.00
η	57.8	28.9	13.7	2.11	0.048	1.00
m*h	31.9	16.0	16.8	0.95	0.353	1.00
m* η	17.1	8.6	16.8	0.51	0.616	1.00
h* η	58.3	29.1	16.8	1.74	0.099	1.00
m*h* η	-51.1	-25.5	20.5	-1.24	0.229	1.00

The values of the regression coefficients are denoted as constants in the Term column of the table. The values of the coefficients are listed in the “Coef” column. Column T represents the t-distribution value of the considering variables; column P lists the probability (p) (p-value) when testing the statistical hypothesis about the possibility that the coefficients equal zero. A (p) value greater than the significance level $\alpha = 0.05$ indicates that the existence of the corresponding coefficient is not statistically significant. The independent variables that have a very strong influence are (m), (h). The (p) value for these variables is less than 0.001, so Minitab displays the value 0.000. The variable (η) with p-value equal to 0.048 has a weaker influence than the above two variables on the objective function (a). In the two-level and three-level interaction factors, both p-values greater than 0.05 are weak effects. The table displays the regression model evaluation parameters. The decision coefficients r^2 (denoted as R-Sq) and r^2_{adj} (denoted as R-sq (adj)) are 92.41% and 89% respectively, which are greater than 90%, proving that the model is appropriate with the data.

Regression Equation in Uncoded Units:

$$a = 18762 - 2112 m - 31647 h - 55.7 \eta + 4229 m*h + 6.94 m*\eta + 103.9 h*\eta - 12.8 m*h*\eta$$

3.4 Experiment analysis for factors affecting rapping force (F)

Screening design: According to the number of variables to be investigated and the cost and time requirements for the experiment, the L9 type of experiment design is selected as experimental plan for the screening experiment. In order to improve the reliability of the experiments, repeat some selected experiments one more time if necessary. Thus, the total number of experiments to be carried out is 12 experiments. The statistical analysis technique will allow evaluation of the influence of the variables considered on the output function as well as the interaction effect between them. Multivariate regression technique is used to determine the relationship between variables and the objective function.

Table 10. Input parameters

Parameter	Symbol	Unit	Value level		
			1	2	3
Hammer mass	m	kg	6	7	8
Drop height between hammer center and impact point	h	m	0.49	0.53	0.57

Dust concentration	η	(mg/Nm ³)	250	300	350
--------------------	--------	-----------------------	-----	-----	-----

3.5 Identify the main factors affecting rapping force (F)

Experimental matrix and result for dust removal acceleration

Table 11. Experimental matrix and result for dust removal acceleration

No.	m (kg)	h (m)	η (mg/Nm ³)	Rapping force F
1	6	0.49	250.00	472.317
2	6	0.53	300.00	462.541
3	6	0.57	350.00	519.022
4	7	0.49	300.00	481.322
5	7	0.53	350.00	517.601
6	7	0.57	250.00	511.483
7	8	0.49	350.00	532.196
8	8	0.53	250.00	511.377
9	8	0.57	300.00	551.140
10	8	0.57	350.20	549.200
11	8	0.57	349.15	516.200
12	8	0.57	350.15	597.200

Main factor affecting the rapping force (F) plot

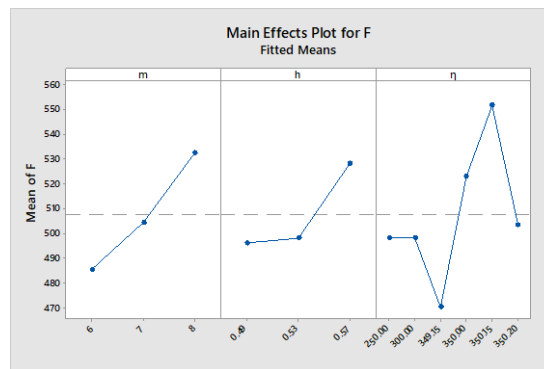


Fig. 5. Main factor affecting the rapping force (F) plot

On the chart in Figure 6, Minitab uses the significance level value α to draw the limit line (with coordinate 4.303 on the graph) of the reversed null hypothesis area. The factors corresponding to the bar that exceed the right of the limit line are values that have a significant effect. The influence values (standardized) are presented as

horizontal bars. The factors corresponding to the bar represented to the right of the limit line are values with significant influence. The factors represented to the left of the limit line are weakly influential. The graph shows that all factors have a negligible influence on F. Specifically, independent parameter (m) has the greatest influence on the rapping force F followed by (h) and then (m).

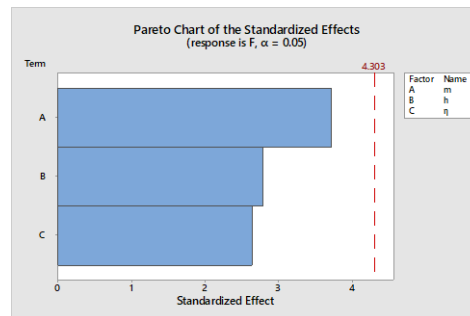


Fig. 6. Main factor affecting the rapping force (F) plot

Regression Equation in Uncoded Units:

$$F = 14 + 31.7m + 678h + 24m.h$$

ANOVA for Regression

Table 12. Analysis of Variance

Source	DF	Adj SS	Adj MS	F-Value	P-Value
Model	7	11653.3	1664.76	1.91	0.278
Linear	3	7860.9	2620.30	3.00	0.158
m	1	3320.3	3320.28	3.81	0.123
h	1	1897.1	1897.08	2.18	0.214
η	1	273.8	273.81	0.31	0.605
2-Way Interactions	3	380.2	126.74	0.15	0.928
m*h	1	11.2	11.16	0.01	0.915
m*η	1	51.8	51.82	0.06	0.819
h*η	1	31.0	31.03	0.04	0.860
3-Way Interactions	1	611.7	611.67	0.70	0.449
m*h*η	1	611.7	611.67	0.70	0.449
Error	4	3488.7	872.19		
Total	11	15142.0			

The analysis of variance shows that the probability (p) value corresponding to the Main effects is 0.158. Therefore, the effects of the variables are insignificant. Two-way interactions (2-way Interactions) is with a p-value of 0.928 and 3-way interactions (3-way Interactions) is with a p-value of 0.449 which is much larger than the α

level (0.05). Therefore, it can be asserted that the variables have a relatively small interaction effect.

3.6 Experiment planning 3^3

After the exploration step, it can be confirmed that the two main factors affecting the rapping force (F) are the hammer mass (m), the hammer dropping height (h). Experiment design L27 is applied.

Table 13. Experimental matrix L27 and measuring results of force F

No.	Variable		Coded variable		Average acceleration
	m	h	X1	X2	a
1	6	0.49	-1	-1	472.32
2	6	0.49	-1	-1	453.42
3	6	0.49	-1	-1	469.32
4	6	0.53	-1	0	481.81
5	6	0.53	-1	0	462.54
6	6	0.53	-1	0	492.54
7	6	0.57	-1	1	511.79
8	6	0.57	-1	1	517.02
9	6	0.57	-1	1	519.02
10	7	0.49	0	-1	486.18
11	7	0.49	0	-1	481.32
12	7	0.49	0	-1	500.77
13	7	0.53	0	0	492.95
14	7	0.53	0	0	497.88
15	7	0.53	0	0	517.60
16	7	0.57	0	1	511.48
17	7	0.57	0	1	501.25
18	7	0.57	0	1	526.83
19	8	0.49	1	-1	506.85
20	8	0.49	1	-1	491.65
21	8	0.49	1	-1	532.20
22	8	0.53	1	0	511.38
23	8	0.53	1	0	485.81
24	8	0.53	1	0	517.60
25	8	0.57	1	1	558.14

26	8	0.57	1	1	551.14
27	8	0.57	1	1	562.47

On the basis of the experimental matrix L27, uses Minitap to set up the equation $F=f(m,h)$ and graph (Figure 7).

3.7 Analyze the influence of factors to F

From the experimental results, establish the Pareto chart (Figure 7).

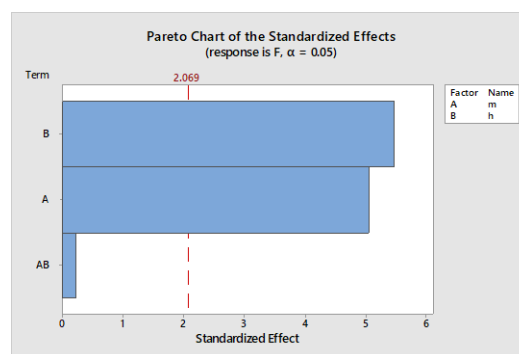


Fig. 7. Pareto chart of the influence of factors on F

On the graph in Figure 7, Minitab uses the significance level value α to indicate the limit line (with coordinates 2.068 on the graph) of the reversed null hypothesis area. The influence values (standardized) are presented as horizontal bars. The factors corresponding to the bar that exceed the right of the limit line, (m) and (h), have a great influence on (F), The factor represented to the left of the limit line has no significant effect.

Analysis of Variance and Regression Equation

Table 14. Analysis of Variance

Source	DF	Adj SS	Adj MS	F-Value	P-Value
Model	3	13743.6	4581.21	18.53	0.000
Linear	2	13732.2	6866.08	27.77	0.000
m	1	6326.2	6326.16	25.58	0.000
h	1	7406.0	7406.01	29.95	0.000
2-Way Interactions	1	11.5	11.46	0.05	0.831
m*h	1	11.5	11.46	0.05	0.831
Error	23	5687.4	247.28		
Lack-of-Fit	5	2642.3	528.45	3.12	0.033
Pure Error	18	3045.1	169.17		

Total	26	19431.0			
-------	----	---------	--	--	--

Table 15. Coded Coefficients

Term	Effect	Coef	SE Coef	T-Value	P-Value	VIF
Constant		504.20	3.03	166.61	0.000	
m	37.49	18.75	3.71	5.06	0.000	1.00
h	40.57	20.28	3.71	5.47	0.000	1.00
m*h	-1.95	-0.98	4.54	-0.22	0.831	1.00

The values of the regression coefficients are denoted as constants in the “Term” column of the table. The values of the coefficients are listed in the “Coef” column. Column T represents the t-distribution value of the quantity in question; column P lists the probability p (p-value) when testing the statistical hypothesis about the possibility that the coefficients equal zero. A (p) value greater than the significance level $\alpha = 0.05$ indicates that the existence of the corresponding coefficient is not statistically significant. The independent variables that have very strong influence are (m), (h). The (p) value for these variables is less than 0.001, so Minitab displays the value 0.000. In the two-level interaction factors, p-values greater than 0.05 are all weak effects.

Regression Equation in Uncoded Units:

$$F = 14 + 31.7m + 678h + 24m.h$$

From the experimental regression equation shows:

Independent parameters (h) and (m) have the greatest influence on the rapping force (F) followed by the interaction between (h) and (m).

Construction of tensile and fatigue curves for discharge electrode frames

Tensile strength test with specimen conforms to TCVN 4169-85 standard “Steel materials - Test methods”. Tensile test graph of CT3 steel discharge frame (Figure 8), Experimental fatigue curve of discharge frame (Figure 9):

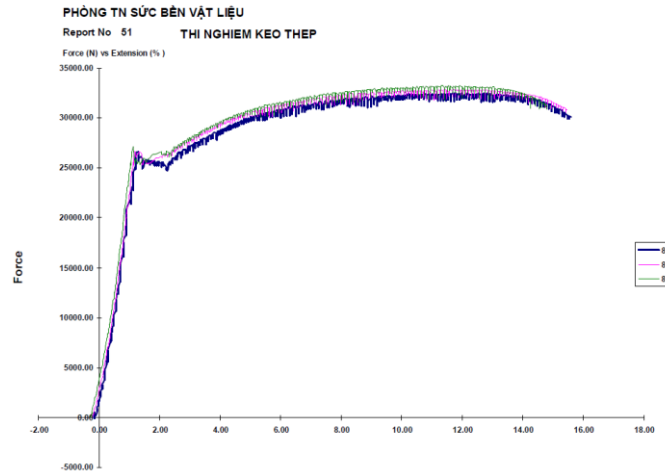


Fig. 8. Tensile test result for CT3 steel

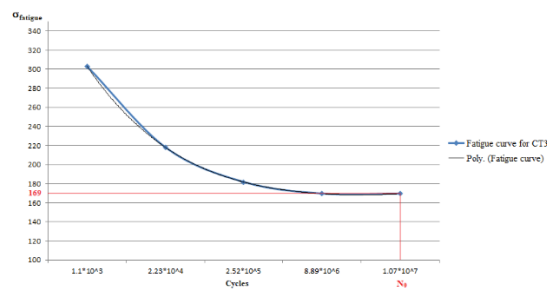


Fig. 9. CT3 steel discharge frame fatigue curve – test on standard test piece

Table 16. Fatigue test result for CT3 steel

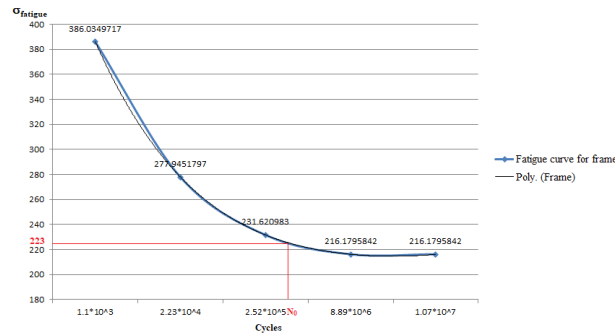
Test no	Test wt. (kg)	Moment of inertia (cm ⁴)	No. of cycles	No. of cycles	fatigue stress of test piece (kg/cm ²)	Fatigue stress of test piece (MPa)
1	25	0.039626254	1100	$1.1 \cdot 10^3$	3028.295301	302.8295301
2	18	0.039626254	22300	$2.23 \cdot 10^4$	2180.372616	218.0372616
3	15	0.039626254	252000	$2.52 \cdot 10^5$	1816.97718	181.697718
4	14	0.039626254	8890000	$8.89 \cdot 10^6$	1695.845368	169.5845368
5	14	0.039626254	10700000	$1.07 \cdot 10^7$	1695.845368	169.5845368

From the above theoretical bases, a set of fatigue stress parameters can be calculated to establish a fatigue curve for the discharge frame. By calculation, the similarity factor is $\text{const}=1.27476$. Fatigue stress parameters for the discharge frame was developed according to Table 17.

Table 17. Parameters for experimental fatigue curves for discharge frames

Fatigue stress of test piece (MPa)	Similarity ratio	Fatigue stress of frame (MPa)
302.8295301	1.27476	386.0349717
218.0372616	1.27476	277.9451797
181.697718	1.27476	231.620983
169.5845368	1.27476	216.1795842
169.5845368	1.27476	216.1795842

From Table 18, the fatigue curve of the discharge frame was established (Figure 10).

**Fig. 10.** Experimental fatigue curve for the discharge frame

4 Scientific discussion of the achieved results

The experiments the following discussion have been achieved:

- Applying simulation software on the experimental curve have found the maximum stress on the discharge electrode frame: $\sigma_{\max}=222,945$ N (223 N);
- Determined the expected life of the discharge frame based on the number of rapping cycles is $N_0 \sim 2.52 \times 10^5$ cycles (equivalent to minimum of ~8.75 years of operation);
- Compared to the allowable tensile stress of the discharge frame made of CT3, the tested tensile stress of CT3 steel $[\sigma_{\text{ch_CT3}}]=328.17$ MPa and meeting the allowable stress for the collecting plates made of CT0 steel with $[\sigma_{\text{ch_CT0}}]=304.23$ MPa (according standard GOST-3SP/PS 380/94). This means that the rapping force (F) meets the durability of the discharge frame while creates the required dust removal acceleration (a) and at the same time is suitable with the allowable stress of the collecting electrode plates.

5 Conclusion

On the basis of experimental results, a matrix $3^3 = 27$ has been established with 3 input parameters: hammer mass (m), hammer drop height (h) and inlet dust concentra-

tion (η), satisfying the output criteria are the dust removal acceleration (a) and the appropriate rapping force (F) of the hammer. From which, two important empirical regression equations have been established, meeting the objectives:

$$a = 18762 - 2112 m - 31647 h - 55.7 \eta + 4229 m.h + 6.94 m.\eta + 103.9 h.\eta - 12.8 m.h.\eta$$

$$F = 14 + 31.7m + 678h + 24m.h$$

The experiment results show that, compared with the ultimate tensile stress of the CT3 steel discharge frame, the tensile stress $[\sigma_{\max}] = 222.945$ MPa due to the impact of rapping force $F = 558.14$ N with a hammer mass of 8 kg and a drop height of $h = 0.57$ m, meets the allowable strength of the discharge frame CT3 steel $\sigma_{\text{ch_CT3}} = 328.17$ MPa, creates the dust removal acceleration and satisfies the allowable tensile strength of the collecting plate CT0 Steel $\sigma_{\text{ch_CT0}} = 304.23$ MPa (GOST-3SP/PS 380/94).

Thus, the obtained results satisfy the multi-objective requirements of the research which, with the rapping force (F) to meet the durability of the discharge frame, creating the dust removal acceleration (a), and at the same time ensuring the durability of the collecting plate.

References

1. T. Yamamoto, H.R. Velkoff, Electrohydrodynamics in an electrostatic precipitator. In: Journal of Fluid Mechanics, Volume 108, 1 – 18 (1981).
2. TCVN 4169 “Metals - Method of multi-cycle and small-cycle fatigue testing”.
3. Nguyễn Tien Sy, Study on the influence of some technical parameters of electrostatic precipitator rapping system on dust removal ability, PhD Thesis (2020).
4. N.A. Tung, H.V. Got, N.T. Sy, N.D. Toan, Empirical Study on the Relationship between Cyclic Rapping Force and the Lifespan of Discharge Electrode Frames in Dust Filter Chambers. In: European Chemical Bulletin, ISSN 2063-5346, 2146-2157 (2023).
5. Писаренко Г.С., Справочник по сопротивлению материалов. In: НАУКОВА ДУМКА (1976).
6. С.В.Серепенен, В.П. Когаев, Несущая способность и Расчёты деталей машин на прочность. In: Москва “машиностроение” (1975).
7. S.H. Kim, K.W. Lee, Experimental study of electrostatic precipitator performance and comparison with existing theoretical prediction models. In: Journal of Electrostatics, Volume 48, Issue 1, 3-25 (1999).
8. Y. Song, Y. Zhang, Study on the influence of electrodes on the collection efficiency during the treatment of welding fume in electrostatic precipitators. In: Journal of Electrostatics, Volume 123, 103808 (2023).